LETTERS
https://doi.org/10.1038/s41566-018-0269-2
nature photonics

Thermal-motion-induced non-reciprocal quantum optical system

Shicheng Zhang[1], Yiqi Hu[1], Gongwei Lin[1]*, Yueping Niu[1]*, Keyu Xia[2,3]*, Jiangbin Gong[4] and Shangqing Gong[1]

Magnetic-free optical non-reciprocal components, such as isolators and circulators, are highly desirable for on-chip optical signal processing[1,2] and quantum networks[3,4]. However, their realization presents a fundamental difficulty due to the Lorentz reciprocity in most optical devices[5]. In this study, we propose and experimentally realize optical non-reciprocity with atoms embedded in a ring cavity at room temperature. Random thermal motion of atoms, in the presence of a unidirectional control field, creates susceptibility–momentum locking, and subsequently a new type of chiral quantum optical system. Furthermore, we demonstrate strong non-reciprocity based on this chiral quantum system in the regime of collectively strong atom–cavity coupling. Our scheme provides a new routine towards the realization of chiral quantum optics and chip-compatible, non-magnetic optical non-reciprocity.

For their wide applications in all-optical signal processing and quantum information processing, non-reciprocal photonic devices without magneto-optical materials have attracted rapidly growing interest. Spatiotemporal modulation of the permittivity of a nonlinear material can generate optical non-reciprocity (ONR) through non-reciprocal frequency conversion of signal light[2,6,7] or by introducing Berry phase[8,9]. Nonlinearity-based ONR has been considered as a good candidate for an optical isolator compatible with a chip platform[10–12]. Due to the dynamic reciprocity, such a kind of nonlinear device is still reciprocal for a weak signal. Their applications are thus limited to cases with large power signals[13]. Alternative strategies have been pursued to break the optical reciprocity, by exploiting a chiral gain in photonic circuits[14,15], 'moving' Bragg mirrors[16], cold atomic Bragg lattices[17], optomechanical systems[18–21] or synthesized magnetic fields[18,22–24]. As an exciting development, chiral quantum optics offers a novel way to realize the ONR even in the quantum regime[25–28].

The inevitable random thermal motion of atoms normally washes out the desired quantum effects and typically plays a negative role in the quantum manipulation of atoms[29–31]. Here, counterintuitively, we exploit the thermal motion as a useful resource to create a non-reciprocal quantum optical system. In our scheme, thermal motion causes 'susceptibility–momentum locking' in atoms (that is, a probe-direction-dependent response assisted by a unidirectional control laser field). This chiral response of atoms, when operating in the collectively strong coupling regime (CSCR), induces the ONR. We perform a proof-of-concept experiment to demonstrate the ONR with an ensemble of warm rubidium (Rb) atoms strongly coupled to a ring cavity, enabling optical isolation without magnetic fields. Our experiment demonstrates the possibility of using microscopic random thermal motion as a tool for the quantum control of optical fields.

The idea of creating a chiral quantum optical system based on the thermal motion of atoms is schematically depicted in Fig. 1a, b. In the absence of the atomic thermal motion (shown in Fig. 1a), a strong control field drives the atomic transition $|2\rangle \leftrightarrow |3\rangle$ with a detuning Δ_c. A weak probe field couples the transition $|1\rangle \leftrightarrow |3\rangle$ with a detuning Δ_p. The susceptibility of the atomic system for the probe field is independent of its propagation direction. However, when taking into account the thermal motion of the atoms, the atomic response becomes chiral due to the direction-dependent microscopic Doppler shift, mediated by the unidirectional propagation of the control field (see Fig. 1b). Here, we account only for the longitudinal Doppler effect along the laser beam direction, because the transverse Doppler effect is negligible. When the probe laser beam co-propagates with the control beam, the microscopic Doppler shifts 'seen' by the moving atoms have the same sign, and thus their effects on the two-photon detuning $\Delta_c - \Delta_p$ are cancelled. By contrast, when these two laser beams propagate along opposite directions, the Doppler shifts are of the opposite signs instead, and their impact on $\Delta_c - \Delta_p$ is thus enhanced. For the co- and counter-propagation cases, the respective susceptibilities[29–31] χ_{co} and χ_{cou} are found to be (details in Supplementary Information)

$$\chi_{co} = \int_{-\infty}^{\infty} \frac{-iN\,|g|^2\,D(v)}{\gamma_3 + i(\Delta_p + kv) + \frac{\Omega_c^2}{\gamma_{12} + i\Delta_p}}\mathrm{d}v$$
$$\chi_{cou} = \int_{-\infty}^{\infty} \frac{-iN\,|g|^2\,D(v)}{\gamma_3 + i(\Delta_p + kv) + \frac{\Omega_c^2}{\gamma_{12} + i(\Delta_p + 2kv)}}\mathrm{d}v \quad (1)$$

where Ω_c is the Rabi frequency of the control field, g is the single-photon coupling rate for the probe field, γ_3 is the spontaneous decay rate associated with the state $|3\rangle$, γ_{12} is the dephasing rate between the two ground states of $|1\rangle$ and $|2\rangle$, k is the photon wavevector and v is the atomic velocity. $D(v) = \mathrm{e}^{-v^2/v_p^2} / (\sqrt{\pi} v_p)$ is the Maxwell–Boltzmann distribution of velocity, where v_p is the most probable velocity. N is the number of involved atoms. The control field is much stronger than the probe field, such that the state $|1\rangle$ is mostly populated, that is $\langle \hat{\sigma}_{11} \rangle \approx 1$. Clearly, the susceptibility of atoms, according to equation (1), is chiral as a result of the random atomic thermal motion and the unidirectionality of the control laser. This

[1]Department of Physics, East China University of Science and Technology, Shanghai, China. [2]National Laboratory of Solid State Microstructures, College of Engineering and Applied Sciences, and School of Physics, Nanjing University, Nanjing, China. [3]Collaborative Innovation Center of Advanced Microstructures, Nanjing University, Nanjing, China. [4]Department of Physics, National University of Singapore, Singapore, Singapore. *e-mail: gwlin@ecust.edu.cn; niuyp@ecust.edu.cn; keyu.xia@nju.edu.cn

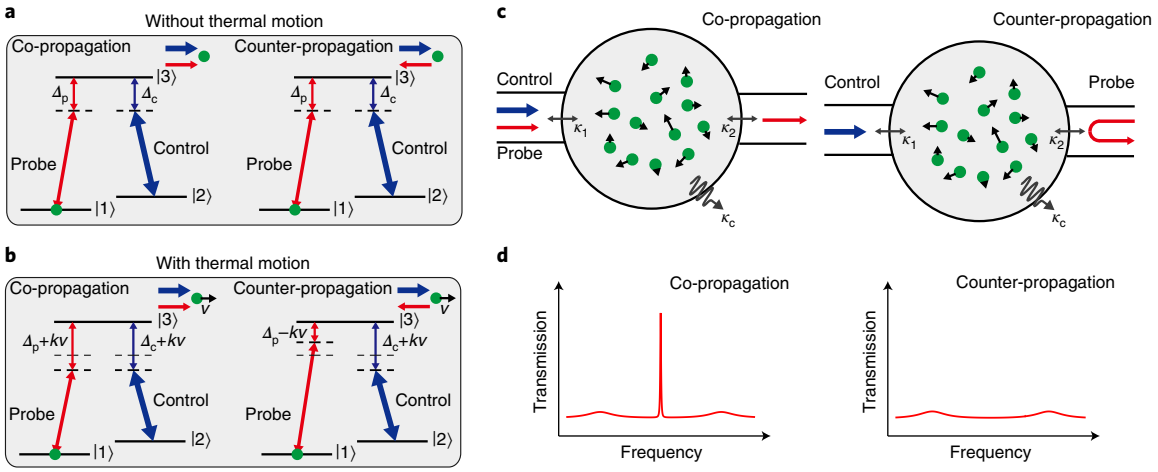

Fig. 1 | Thermal-motion-induced non-reciprocal chiral quantum optical system. a,**b**, Level diagrams of the atomic medium, driven by a strong control field and a weak probe field. **a**, In the absence of thermal motion, the left (right) panel is for the probe field co-propagating (counter-propagating) with the control field. **b**, In the presence of thermal motion, for the atom with a velocity component *v* along the laser beam: the atoms 'see' the same 'microscopic' Doppler shifts in the co-propagation case (left) or the atoms 'see' opposite 'microscopic' Doppler shifts in the counter-propagation case (right). **c**, Schematics for creating optical non-reciprocity with a chiral system embedded in a ring cavity. Left: the probe field passes through the cavity in the co-propagation case. Right: the probe field is reflected from the cavity in the counter-propagation case. **d**, Schematics of transmission spectra for co-propagation (left) and counter-propagation (right) cases.

susceptibility–momentum-locking-induced chirality is essentially different from the chirality caused by the previously studied spin–momentum-locking mechanism[3] in two aspects: the latter requires the direction-locked circular polarization to excite the polarization-dependent dipole transitions; the thermal motion in the latter acts as a 'negative' factor and needs to be avoided as much as possible. By contrast, the atomic thermal motion in our proposal is crucial in achieving the chirality.

Based on the susceptibility–momentum-locking-induced chirality, we shall achieve ONR by simply exploiting a strong collective coupling between a ring cavity and an ensemble of quantum emitters (see Fig. 1c). In our configuration the cavity transmission for the co-propagation (counter-propagation) case is given by

$$T_{\mathrm{co(cou)}} = \left| \frac{\sqrt{\kappa_1 \kappa_2}}{i\Delta_{\mathrm{p}} + \frac{\kappa}{2} + i\chi_{\mathrm{co(cou)}}} \right|^2 \qquad (2)$$

where $\kappa = \kappa_{\mathrm{c}} + \kappa_1 + \kappa_2$, κ_{c} is the cavity intrinsic damping rate, and κ_1 and κ_2 are the coupling rates for the input and output of the probe field, respectively. As schematically shown in Fig. 1d, the transmission spectra show vacuum Rabi splitting (VRS) in the CSCR[31] and depend strongly on the relative direction of probe and control fields. In particular, the transmission near the resonant position is very high in the co-propagation case, whereas it is vanishingly small in the counter-propagation case. Thus, the near-resonance cavity transmission exhibits a strong ONR in the CSCR. Figure 2a,b depicts the theoretical co- and counter-propagation transmissions at $\Delta_{\mathrm{p}} = 0$ versus the control field strength Ω_{c} and the collective coupling strength $\sqrt{N}g$. Clearly, within a wide range of Ω_c and $\sqrt{N}g$, a high transmission is available for the co-propagation case, in sharp contrast to nearly zero transmission for the counter-propagation case. Specifically, very strong ONR can be obtained when $\sqrt{N}g \gg \kappa$. The strong ONR is a result of the combined effects of the susceptibility–momentum-locking-induced chirality and the large VRS in the CSCR. As also shown in Fig. 2a, a high co-propagation transmission can be achieved with a strong control field.

The physical mechanisms behind the emergence of the ONR are twofold. First, in the co-propagation case, thermal motion induces the same 'microscopic' Doppler shifts for the control and probe fields, and thus the two-photon resonance condition can be maintained in the presence of Doppler shifts. As a result, the Λ-type system forms an intracavity electromagnetically induced transparency (EIT), and subsequently dark-state resonance, leading to a high transmission of the probe field[31]. In the counter-propagation case, however, thermal motion induces opposite 'microscopic' Doppler shifts, destroying the dark-state resonance condition. Second, in the CSCR, the strong collective coupling between the cavity mode and atoms induces a large VRS, strongly suppressing the transmission of the probe field counter-propagating with the control field. The random atomic thermal motion thus generates the susceptibility–momentum-locking and then triggers optical non-reciprocity via EIT.

In laser cooling of thermal atoms below the one-photon recoil energy, the so-called velocity-selective coherent population trapping was also built on opposite microscopic Doppler shifts of two counter-propagating laser beams[32]. There the objective is to trap sufficiently slow-moving atoms in the dark state. Here, in our ONR scheme, the cancelled or enhanced effects of the Doppler shifts for two co-propagating or counter-propagating laser beams are used to control the transmission of one of the two laser beams. That is, the propagation direction of the weak probe field is selected by the dark-state resonance condition for EIT. The tremendous impact of the microscopic Doppler effects on laser cooling[32] suggests that our approach to non-reciprocal quantum optics can be powerful as well. Note also that the 'macroscopic' Doppler effect in an accurately synthesized 'moving' Bragg mirror[16] or a cold atomic Bragg lattice[17] has been exploited to induce the ONR. These two previous approaches are markedly different from ours. The key difference is that our scheme makes use of the 'microscopic' Doppler effect of random atomic thermal motion, an effect that naturally exists in warm atoms but needs to be avoided in those previous works[16,17].

Our proof-of-concept experiment demonstrating the chirality and the ONR was performed with warm ^{87}Rb atoms in a three-mirror ring cavity. The ring cavity has a path length of ~49 cm and a

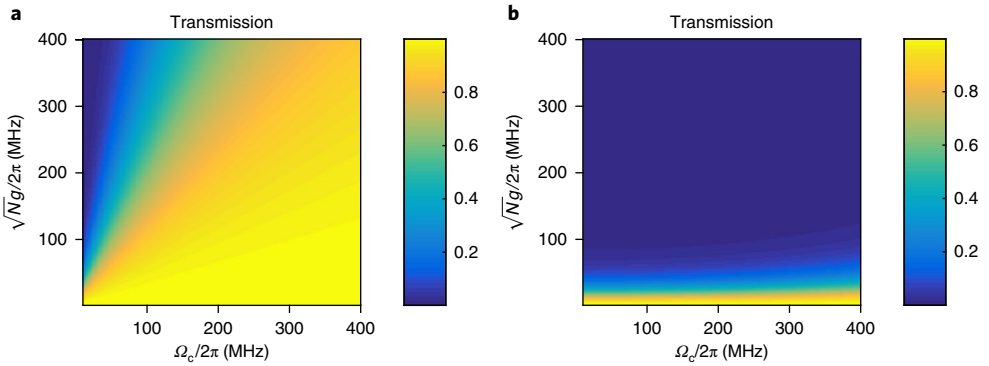

Fig. 2 | Non-reciprocal transmission of the chiral quantum optical system inside a ring cavity. a,**b**, Normalized transmission as a function of the control field strength Ω_c and the collective coupling strength $\sqrt{N}g$ for the co-propagation (**a**) and counter-propagation (**b**) cases. The parameters are $\Delta_c=\Delta_p=0$ MHz, $\{\kappa_1/2\pi, \kappa_2/2\pi, \kappa_c/2\pi\}=\{0.5, 4, 6\}$ MHz, $\gamma_3/2\pi=10$ MHz, $\gamma_{12}/2\pi=0.8$ MHz, $\lambda=2\pi/k=795$ nm and $T=55$ °C.

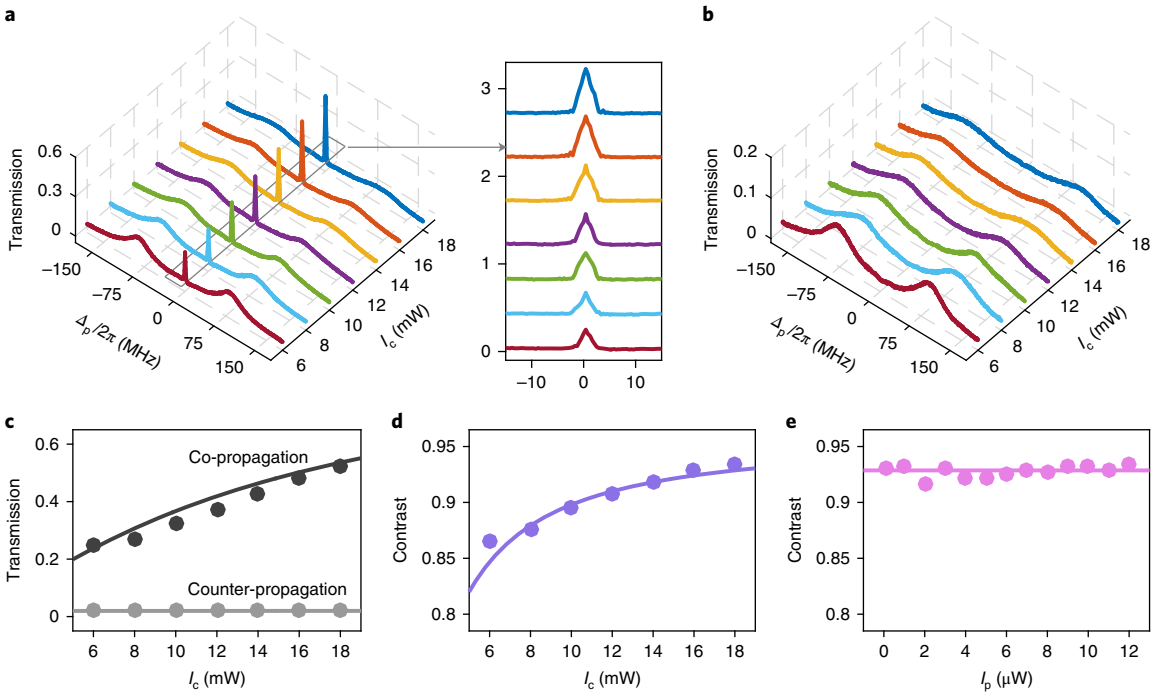

Fig. 3 | Experimental observation of non-reciprocal transmission with warm atoms. a,**b**, Normalized transmission spectra of the probe field at different control field power I_c for the co-propagation (**a**) and counter-propagation (**b**) cases. **c**, Normalized on-resonance transmission versus the control field power. The black (grey) dots are for the co-propagation (counter-propagation) case. **d**, Transmission contrast versus the control field power with a fixed probe field power $I_p=12$ μW. **e**, Transmission contrast versus the probe field power with a fixed control field power $I_c=18$ mW. The solid curves in **c**–**e** represent the theoretical results. The parameters for the theoretical plots are chosen to be the same as those in Fig. 2.

finesse of 60 (cavity mode damping rate $\kappa/2\pi\simeq10$ MHz). The main experimental results are shown in Fig. 3a–e. Figure 3a,b are the measured co- and counter-propagation transmission spectra of the probe field with a fixed power of $I_p=12$ μW and a varying control field power I_c at a temperature of 55 °C (the system is clearly in the CSCR in this condition, see Supplementary Information). The near-resonance transmission is high in the co-propagation case (see also the inset of Fig. 3a) but nearly zero in the counter-propagation case. In particular, the on-resonance transmission versus the power of the control laser is shown in Fig. 3c. There the co-propagation transmission increases from 25% to 53%, whereas the counter-propagation transmission is always vanishingly small when the control laser power increases from 6 mW to 18 mW.

The above-observed strong ONR can be used for optical isolation. To characterize the possible optical isolation performance, we next evaluate the contrast of the two transmission cases using $\eta=(T_{co}-T_{cou})/(T_{co}+T_{cou})$ (ref. [16]). Figure 3d presents the contrast η versus the control field power. Limited by our experimental condition, we can scan the control field power only from 6 mW to 18 mW. Accordingly, the contrast increases from 0.87 to 0.93. If a higher control field power is available, a stronger contrast is expected from our theory. In addition, for a fixed $I_c=18$ mW, the contrast η versus the probe field power I_p is also investigated in Fig. 3e to demonstrate the stability of the obtained ONR. It is found that the contrast remains almost unchanged when the power varies over two orders of magnitude; namely, decreasing from 12 μW to 150 nW.

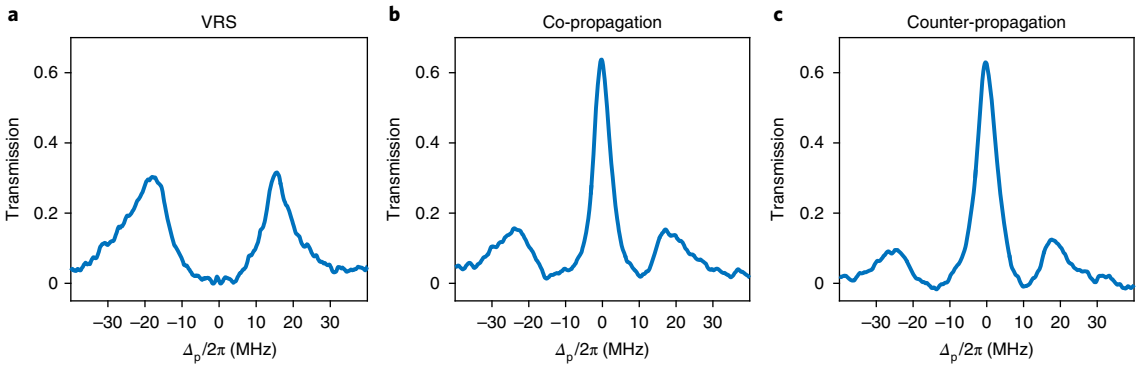

Fig. 4 | Experimental observation of reciprocal transmission with cold atoms. a, Normalized transmission spectra of the probe field without the control field, exhibiting VRS. **b**,**c**, Normalized transmission spectra of the probe field for the co-propagation (**b**) and counter-propagation (**c**) cases. Here the probe field power is fixed at 0.5 μW and the control field power is 6 mW. The temperature of cold atoms trapped in the magneto-optical trap is approximately 200 μK.

Remarkably, all the experimental data (dots) are fitted well by our theoretical results (solid curves) on using the experimentally measured VRS to extract the value of $\sqrt{N}g$, thus fully confirming our physical insights and theoretical analysis above.

We have also extensively investigated the effects of varying temperature on both the transmission contrast and the transmission itself—two important factors for the design of optical devices. For our current experimental platform, we obtain both high transmission contrast and appreciable transmission in the co-propagation case, for a considerable temperature window around 55 °C; for example from 50 °C to 60 °C (see the Supplementary Information). To double-confirm the essential role of the microscopic Doppler effect in our ONR scheme, we have also carried out separate experiments for cold atoms at temperatures of approximately 200 μK captured by a two-dimensional magneto-optical trap. The transmission spectra for cold atoms are reported in Fig. 4. The CSCR for cold atoms is evidenced by the clearly separated transmission peaks in Fig. 4a without the control field. In this CSCR, Fig. 4b,c shows that the transmission spectra of the probe field in the presence of a control field are almost perfectly reciprocal, with the power of the probe and the control fields in the same range as in our experiments for warm atoms. Such a set of control experiments firmly testify that the above optical non-reciprocity for warm atoms is indeed induced by the thermal motion of the atoms.

In summary, making use of the random thermal motion of warm atoms, we have realized a non-reciprocal quantum optical system. Atomic thermal motion, which is a nuisance for most applications so far, plays a 'constructive' role in the successful creation of the ONR here. A proof-of-principle experiment has been performed with warm Rb atoms in a ring cavity, demonstrating that our simple scheme can be operated under practical conditions with a wide parameter range, and can indeed be highly useful in the design of optical non-reciprocal devices. Because EIT has been performed in warm atoms at the single-photon level[33], the chiral optical system proposed and demonstrated here has the potential to work with a very weak probe field, even for a single-photon pulse. Furthermore, since warm atoms can be trapped in one-dimensional waveguides (for example, photonic crystal fibres or tapered nanofibres), our proposal may open a new door for integrated chiral photonics.

Data availability

The data that support the plots within this paper and other findings of this study are available from the corresponding authors upon reasonable request.

Received: 31 January 2018; Accepted: 10 September 2018;
Published online: 22 October 2018

References

1. Khanikaev, A. B. & Alù, A. Optical isolators: nonlinear dynamic reciprocity. *Nat. Photon.* **9**, 359–361 (2015).
2. Yu, Z. & Fan, S. Complete optical isolation created by indirect interband photonic transitions. *Nat. Photon.* **3**, 91–94 (2009).
3. Lodahl, P. et al. Chiral quantum optics. *Nature* **541**, 473–480 (2017).
4. Cirac, J. I., Zoller, P., Kimble, H. J. & Mabuchi, H. Quantum state transfer and entanglement distribution among distant nodes in a quantum network. *Phys. Rev. Lett.* **78**, 3221–3224 (1996).
5. Jalas, D. et al. What is — and what is not — an optical isolator. *Nat. Photon.* **7**, 579–582 (2013).
6. Estep, N. A., Sounas, D. L., Soric, J. & Alù, A. Magnetic-free non-reciprocity and isolation based on parametrically modulated coupled-resonator loops. *Nat. Phys.* **10**, 923–927 (2014).
7. Kang, M. S., Butsch, A. & Russell, P. S. J. Reconfigurable light-driven opto-acoustic isolators in photonic crystal fibre. *Nat. Photon.* **5**, 549–553 (2011).
8. Sounas, D. L., Caloz, C. & Alù, A. Giant non-reciprocity at the subwavelength scale using angular momentum-biased metamaterials. *Nat. Commun.* **4**, 2407 (2013).
9. Sounas, D. L. & Alù, A. Angular-momentum-biased nanorings to realize magnetic-free integrated optical isolation. *ACS Photon.* **1**, 198–204 (2014).
10. Fan, L. et al. An all-silicon passive optical diode. *Science* **335**, 447–450 (2012).
11. Chang, L. et al. Parity–time symmetry and variable optical isolation in active–passive-coupled microresonators. *Nat. Photon.* **8**, 524–529 (2014).
12. Peng, B. et al. Parity–time-symmetric whispering-gallery microcavities. *Nat. Phys.* **10**, 394–398 (2014).
13. Shi, Y., Yu, Z. & Fan, S. Limitation of nonlinear optical isolators due to dynamic reciprocity. *Nat. Photon.* **9**, 388–392 (2015).
14. Hua, S. et al. Demonstration of a chip-based optical isolator with parametric amplification. *Nat. Commun.* **7**, 13657 (2016).
15. Zheng, Y. et al. Optically induced transparency in a micro-cavity. *Light Sci. Appl.* **5**, e16072 (2016).
16. Wang, D.-W. et al. Optical diode made from a moving photonic crystal. *Phys. Rev. Lett.* **110**, 093901 (2013).
17. Horsley, S. A. R., Wu, J.-H., Artoni, M. & La Rocca, G. C. Optical nonreciprocity of cold atom Bragg mirrors in motion. *Phys. Rev. Lett.* **110**, 223602 (2013).
18. Fang, K. et al. Generalized non-reciprocity in an optomechanical circuit via synthetic magnetism and reservoir engineering. *Nat. Phys.* **13**, 465–471 (2017).
19. Hafezi, M. & Rabl, P. Optomechanically induced non-reciprocity in microring resonators. *Opt. Express* **20**, 7672–7684 (2012).
20. Shen, Z. et al. Experimental realization of optomechanically induced non-reciprocity. *Nat. Photon.* **10**, 657–661 (2016).
21. Ruesink, F., Miri, M.-A., Alù, A. & Verhagen, E. Nonreciprocity and magnetic-free isolation based on optomechanical interactions. *Nat. Commun.* **7**, 13662 (2016).
22. Fang, K., Yu, Z. & Fan, S. Realizing effective magnetic field for photons by controlling the phase of dynamic modulation. *Nat. Photon.* **6**, 782–787 (2012).
23. Fang, K., Yu, Z. & Fan, S. Photonic Aharonov–Bohm effect based on dynamic modulation. *Phys. Rev. Lett.* **108**, 153901 (2012).

24. Tzuang, L. D., Fang, K., Nussenzveig, P., Fan, S. & Lipson, M. Non-reciprocal phase shift induced by an effective magnetic flux for light. *Nat. Photon.* **8**, 701–705 (2014).
25. Sayrin, C. et al. Nanophotonic optical isolator controlled by the internal state of cold atoms. *Phys. Rev. X* **5**, 041036 (2015).
26. Scheucher, M., Hilico, A., Will, E., Volz, J. & Rauschenbeutel, A. Quantum optical circulator controlled by a single chirally coupled atom. *Science* **354**, 1577–1580 (2016).
27. Xia, K. et al. Reversible nonmagnetic single-photon isolation using unbalanced quantum coupling. *Phys. Rev. A* **90**, 043802 (2014).
28. Söllner, I. et al. Deterministic photon–emitter coupling in chiral photonic circuits. *Nat. Nanotech.* **10**, 775–778 (2015).
29. Gea-Banacloche, J., Li, Y.-Q., Jin, S.-Z. & Xiao, M. Electromagnetically induced transparency in ladder-type inhomogeneously broadened media: theory and experiment. *Phys. Rev. A* **51**, 576–584 (1995).
30. Xiao, M., Li, Y.-Q., Jin, S.-Z. & Gea-Banacloche, J. Measurement of dispersive properties of electromagnetically induced transparency in rubidium atoms. *Phys. Rev. Lett.* **74**, 666–669 (1995).
31. Wu, H., Gea-Banacloche, J. & Xiao, M. Observation of intracavity electromagnetically induced transparency and polariton resonances in a Doppler-broadened medium. *Phys. Rev. Lett.* **100**, 173602 (2008).
32. Aspect, A., Arimondom, E., Kaiser, R., Vansteenkiste, N. & Cohen-Tannoudj, C. Laser cooling below the one-photon recoil energy by velocity-selective coherent population trapping. *Phys. Rev. Lett.* **61**, 826–829 (1988).
33. Höckel, D. & Benson, O. Electromagnetically induced transparency in cesium vapor with probe pulses on the single-photon level. *Phys. Rev. Lett.* **105**, 103605 (2010).

Acknowledgements

This work was supported by the National Key Research and Development Program of China (grant no. 2017YFA0303703), the National Natural Science Foundation of China (grant nos. 11474092, 11774089 and 11674094) and Shanghai Natural Science Foundation (grant nos. 17ZR1442700 and 18ZR1410500).

Author contributions

G.L., Y.N. and K.X. contributed to the original idea, and supervised the experiment. S.Z. and Y.H. conducted the experiment and partly contributed to refining the idea. They contributed equally to this work. S.G. supervised the whole project. All authors contributed to discussions of the results and writing of the manuscript.

Competing interests

The authors declare no competing interests.

Additional information

Supplementary information is available for this paper at https://doi.org/10.1038/s41566-018-0269-2.

Reprints and permissions information is available at www.nature.com/reprints.

Correspondence and requests for materials should be addressed to G.L. or Y.N. or K.X.

Publisher's note: Springer Nature remains neutral with regard to jurisdictional claims in published maps and institutional affiliations.